Title

Transcription Factor Zhx2 Deficiency Reduces Atherosclerosis and Promotes Macrophage Apoptosis in Mice.

Journal

Arteriosclerosis, thrombosis, and vascular biology, 38(9)

ISSN

1079-5642

Authors

Erbilgin, Ayca
Seldin, Marcus M
Wu, Xiuju
et al.

Publication Date

2018-09-01

DOI

10.1161/atvbaha.118.311266

Peer reviewed

Published in final edited form as:

Arterioscler Thromb Vasc Biol. 2018 September ; 38(9): 2016–2027. doi:10.1161/ATVBAHA.118.311266.

Transcription factor *Zhx2* deficiency reduces atherosclerosis and promotes macrophage apoptosis in mice

Ayca Erbilgin[*,1,2], **Marcus M. Seldin**[*,1,2], **Xiuju Wu**[*,1,2], **Margarete Mehrabian**[*,1,2], **Zhiqiang Zhou**[1,2], **Hongxiu Qi**[1,2], **Keeyon S. Dabirian**[1,2], **René R. Sevag Packard**[1], **Wei Hsieh**[2], **Steven J. Bensinger**[2], **Satyesh Sinha**[†,1,3], and **Aldons J. Lusis**[†,1,2,4]

[1]Department of Medicine, David Geffen School of Medicine, University of California, Los Angeles, CA 90095, USA

[2]Department of Microbiology, Immunology and Molecular Genetics, University of California, Los Angeles, CA 90095, USA

[3]Department of Internal Medicine, Charles R. Drew University of Medicine and Science, Los Angeles, CA 90059, USA

[4]Department of Human Genetics, David Geffen School of Medicine, University of California, Los Angeles, CA 90095, USA

Abstract

Objective—To determine the basis of resistance to atherosclerosis of inbred mouse strain BALB/cJ.

Approach and Results—BALB/cJ mice carry a naturally occurring null mutation of the gene encoding the transcription factor *Zhx2*, and genetic analyses suggested that this may confer resistance to atherosclerosis. On a hyperlipidemic $Ldlr^{-/-}$ background BALB/cJ mice carrying the mutant allele for *Zhx2* exhibited up to a 10-fold reduction in lesion size as compared to an isogenic strain carrying the wild-type allele. Several lines of evidence, including bone marrow (BM) transplantation studies, indicate that this effect of *Zhx2* is mediated in part by monocytes/macrophages, although non-BM-derived pathways are clearly involved as well. Both in culture and in atherosclerotic lesions, macrophages from *Zhx2* null mice exhibited substantially increased apoptosis. *Zhx2* null macrophages were also enriched for M2 markers. Effects of *Zhx2* on proliferation and other BM-derived cells such as lymphocytes were at most modest. Expression microarray analyses identified over 1,000 differentially expressed transcripts between *Zhx2* wild-type and null macrophages. To identify the global targets of *Zhx2*, we performed ChIP-seq studies with the macrophage cell line RAW264.7. The ChIP-seq peaks overlapped very significantly with gene expression and together suggested roles for transcriptional repression and apoptosis.

Conclusions—A mutation of *Zhx2* carried in BALB/cJ mice is responsible in large part for its relative resistance of the strain to atherosclerosis. Our results indicate that *Zhx2* promotes

Corresponding author: Aldons J. Lusis, Department of Medicine/Division of Cardiology, A2-237 Center for the Health Sciences, UCLA, Los Angeles, CA 90095-1679, Phone: 310-825-1359, FAX: 310-794-7345, jlusis@mednet.ucla.edu.

*Co-first authors

†Co-senior authors

macrophage survival and pro-inflammatory functions in atherosclerotic lesions, thereby contributing to lesion growth.

Keywords

Atherosclerosis; zinc-fingers and homeoboxes 2 (*Zhx2*); ChIP-seq; gene expression; macrophage proliferation and apoptosis; BALB/cJ

Subject codes

Atherosclerosis; Genetics; Gene Expression and Regulation; Animal Models of Human Disease; Inflammation

Introduction

In previous genetic studies in mice, we identified a locus with a modest effect on plasma cholesterol and triglyceride levels on chromosome 15 [1] and subsequently used a positional cloning approach involving the analysis of congenic mouse strains to fine map and identify the putative transcription factor *Zhx2* as causal [2, 3]. One of the parental strains employed in the original genetic cross, BALB/cJ, was found to carry a retroviral insertion that rendered the transcript unstable, essentially resulting in a null mutation with little or no functional protein. The same *Zhx2* gene mutation had previously been demonstrated to contribute to reduced silencing of alpha-fetoprotein (AFP) in adult liver in the BALB/cJ strain [4]. A separate substrain of BALB/c, BALB/cByJ, did not carry the *Zhx2* mutation and in genetic crosses between the substrains plasma triglycerides and cholesterol levels segregated with the *Zhx2* gene. *Zhx2* is expressed in a variety of cell types, but we showed using a hepatocyte-specific transgenic expression of *Zhx2* that the effect on plasma lipids is mediated entirely by hepatic *Zhx2* [2]. In addition to its transcriptional role in regulating AFP in hepatocytes, recent studies have shown an involvement of *Zhx2* in hepatocellular carcinoma [5], lymphoma [6, 7] and myeloma [8, 9]. These findings support both the characterization of *Zhx2* as a transcriptional repressor and a tumor suppressor [10].

We now report an analysis of the effects of *Zhx2* expression on atherosclerosis in low density lipoprotein receptor null ($Ldlr^{-/-}$) mice. Our results identify *Zhx2* as a significant regulator of atherosclerosis in part through its effects on bone marrow (BM)-derived cells, although the levels of circulating blood cells were not discernibly affected. *Zhx2* deficiency resulted in a substantial increase in macrophage apoptosis in lesions and an enrichment of M2 markers. We show that *Zhx2* has broad effects on gene expression in macrophages and we identify some of the direct targets of *Zhx2* using ChIP-seq analysis. To determine the mechanistic basis of the effects of *Zhx2* on atherosclerosis, we have examined macrophage proliferation, apoptosis, and inflammatory functions.

Materials and Methods

The data that support the findings of this study are available from the corresponding author upon reasonable request.

Animals

BALB/cJ mice carrying the endogenous *Zhx2*$^{-/-}$ allele (*Zhx2* null) were obtained from the Jackson Laboratory and mated with BALB/cBy *Ldlr*$^{-/-}$ mice with the *Zhx2*$^{+/+}$ allele (wt). Pups heterozygous for the *Zhx2* null mutation and *Ldlr*$^{-/-}$ were then backcrossed with selection at each generation to strain BALB/cJ for 5 generations, and then intercrossed to generate BALB/cJ *Ldlr*$^{-/-}$ mice carrying the *Zhx2* wt, *Zhx2*$^{+/-}$, and *Zhx2* null gentoypes used for experiments. Mice were maintained on a chow diet or a Western diet (Open Source D12079B). For atherosclerosis studies male and female mice were maintained on a chow diet until 8 weeks of age and then placed on a Western diet for 18 or 24 weeks. Adult mice were euthanized using isoflurane in accordance with ARC policies. For in vivo studies we generally used both male and female mice, while for in vitro studies, where sex differences are unlikely to be as important, we generally used one sex depending upon availability.

Genotyping

DNA was isolated from mouse ear or tail tissue using the Qiagen DNeasy kit. Genotyping was performed using PCR (TaKaRa reagents) followed by agarose gel separation of amplified products to determine size. DNA genotyping of blood isolated from bone marrow recipients was performed using Sigma Extract-n-amp kit. *Zhx2* primers: *Zhx2*-F 5′ ACTGTCTCAGCTCATTCCCTGCAA 3′; *Zhx2*-R 5′ AATGCTTCACATGGCACACAGCAG 3′; *Zhx2*-MR 5′ TCTGCCATTCTTCAGGTCCCTGTT 3′; *Ldlr* primers: LDLR-F: 5′ ACCCCAAGACGTGCTCCCAGGATGA 3′, LDLR-Rwt: 5′ CGCAGTGCTCCTCATCTGACTTGT 3′; LDLR-Rko: 5′ AGGTGAGATGACAGGAGATC 3′

Lesion analyses

After euthanization, the chest cavity of the mouse was opened and the vasculature was perfused with PBS. Quantitation of atherosclerotic lesions was determined in the aortic sinus and proximal aorta by sectioning and staining with Oil Red O [11–13], and *en face* analysis was performed on aortic arch and distal aorta as previously described [3]. This study adhered to the guidelines for experimental atherosclerosis studies as described in the AHA Statement [14].

Plasma lipid analysis

Male and female mice were fasted for 4h beginning at 6AM and bled through the retro-orbital vein into microtainer tubes containing 0.5 M EDTA. After centrifugation, plasma was collected and subjected to quantitation of HDL and non-HDL cholesterol and other lipids as previously described [2].

Macrophage collection, treatment, and RNA isolation

Female mice at 16 weeks of age fed a chow diet were injected in the intraperitoneal cavity with 4% Thioglycolate (Brewer Thioglycollate Medium, BD#211716). On the fourth day after injection, macrophages were collected through lavage of the peritoneal cavity using PBS buffer. Collected cells were treated with ACK lysis buffer (Fisher Scientific

BW10-548E) to remove red blood cells and were then cultured overnight in DMEM media with 20% FBS. The next morning the cell culture dishes were rinsed with PBS and RNA from the cell cultures was collected using buffer RLT from the Qiagen RNeasy kit. RNA was isolated with the Qiagen RNeasy kit following the manufacturer's protocol. LPS treatment: after rinse with PBS the morning after cell harvest, media containing 1% FBS was added to cell cultures; LPS at a final concentration of 2 ng/mL was used for the subset of samples to be treated. After 4 hours, RNA from the cell cultures was collected and isolated as above.

Gene expression

cDNA was synthesized with Applied Biosystems High-Capacity cDNA Reverse Transcription Kit. Roche and KAPA Biosystems SYBR green reagents were used for RT-qPCR and reactions were processed on 384-well plates on the Roche LightCycler 480. RT-qPCR primer sequence for *Zhx2*-F: 5′-ACACTGATAGGAAGCTGCCTGGT-3′, *Zhx2*-R: 5′-TCAAATGCCTTTGGCTTCCCTTGG-3′, 36B4-F: 5′-TGAAGCAAAGGAAGAGTCGGAGGA-3′, 36B4-R: 5′-AAGCAGGCTGACTTGGTTGCTTTG-3′. Affymetrix HT Mouse Genome 430 array plates were used for microarray analysis.

Bone marrow transplantation

BM donors were euthanized at approximately 6 weeks of age on the day of the transplant, and BM was collected from the tibias and femurs. All mice were male. Briefly, the bones were flushed with DMEM media into a falcon tube using a syringe. Media containing the flushed bone marrow was kept on ice. After all BM was harvested, the collected media was passed through a 70 μm filter (BD falcon 352350), treated with ACK lysis buffer, and rinsed with fresh DMEM. BM cells were counted and kept on ice; a minimum of 10 million cells were given to each BM recipient (females) were between 6 and 8 weeks of age. On the day of the transplant, recipients were given a dose of 8 Gy radiation using a cesium source, and BM cells were transplanted using tail-vein injection. Mice were maintained in sterile cages with antibiotics in the water and autoclaved food for a four-week recovery period, after which they were placed on a Western diet for 18 weeks.

Colony forming assay

BM stem cells ($2x10^4$) from Zhx2 wt and null mice were cultured in 35mm dish with IMDM (Thermo Fischer Scientific), consisting MethoCult M3234 (Stemcell Technologies) and M-CSF (30ng/ml). Media were changed every 2 days. After twelve days we counted the number of colonies (50 cells or more) in each genotype [15].

T-Cell Experiments

Secondary lymphoid organs (spleen, popliteal and inguinal lymph nodes) were crushed and treated with 1 mg/mL collagenase type 3 (Worthington Biochemical) for 1h. $CD11c^+$ dendritic cells (DCs), regulatory T-cells (Treg) and $CD4^+$ T-cells were isolated using antibodies coated with magnetic beads (Miltenyi Biotec). All DCs were treated with 50 μg/mL mitomycin C (Sigma-Aldrich M4287) and washed. For all T-cell isolations, Zhx2 wt and null isogenic, $Ldlr^{-/-}$ mice on a BALB/cJ background were used. For DC and Treg

isolation, BALB/cByJ were also used. All mice were fed a regular chow diet. Cells were cultured for 72h, and pulsed with 1 μCi ^{3}H-thymidine (Perkin Elmer) for the last 18h. After the 72h incubation, ^{3}H-thymidine incorporation was used to determine T-cell proliferation and activation by scintillation counting. All of the studies resulted in insignificant differences between *Zhx2* wt and null mice (see Suppl. Tables I–V).

Effect of Zhx2 genotype on response to different TLR ligands

Control (wt) or *Zhx2* null BMDM from male mice were plated at 1.5x10^{5} cell/well in 24-well optical imaging black plates (Cellvis, P24-1.5H-N). The next day, cells were treated with TLR2, TRL3, TL4, TRL7/8, or TRL9 ligands for 48 hr. Immediately, prior to imagining, 1.25 μM (final concentration) Calcein-AM (Santa Cruz, SC-203865) was added to each well and incubated for 5 minutes. The plates were then imaged on a Molecular Devices ImageXpress XL. 21 high magnification fluorescence images were captured for each well (21.83% of total well surface area) using a 10x Objective. Cell number was assessed using MetaXpress Software with Powercore. Data represent three independent experiments. For all gene expression analysis, wt control or Zhx2 null BMDM were plated at 3x10^{5} cell/well in 12-well plates. The next day, cells were treated cells were treated with TLR2, TRL3, TL4, TRL7/8, or TRL9 ligands for 6 hr. RNA was isolated and cDNA was synthesized with high-capacity cDNA reverse transcription kit. KAPA SYBR FAST qPCR Master Mix (2X) kit and a LightCycler 480 were used for quantitative RT-PCR. Fold change related to the control group was calculated using 2ΔΔCP method with 36b4 as the reference gene. Primer sequences are listed in Suppl. Table XII. Results represents two independent experiments.

Detection of Ki-67 in atherosclerotic lesions

Immunofluorescence was performed on tissue sections from frozen, OCT-embedded proximal aortas from wt and null male mice. Antibodies to CD68 (MCA1957GA, Biorad), and Ki-67 (ab15580, abcam) were used to detect macrophages, and cell proliferation, respectively. Antibody to CD68 or Ki-67 was detected with AlexaFlour 594 conjugated antibody to rat IgG (Life Technologies) or AlexaFlour 488 conjugated antibody to rabbit IgG (Life technologies). The nuclei were stained with DAPI (Sigma-Aldrich). The quantification of Ki67 staining was done by normalizing the Ki67 positive nuclei colocalized with CD68 to total nuclei numbers in CD68 stained area. We used a Zeiss LSM 880 confocal microscope to visualize the staining.

In vivo 5-Ethynyl-2′-deoxyuridine (EdU) incorporation and detection

Male *Ldlr*$^{-/-}$ mice were maintained on an atherosclerotic diet for 24 weeks. 1.26 mg EdU (from 10mM stock solution) was injected intraperitoneally. Mice were sacrificed 2 hours later and 10μm cryo-sections from frozen, OCT-embedded proximal aortas were prepared. EdU was detected in these tissue sections using the Click-iT™ EdU Alexa Fluor™ 488 Imaging Kit (Invitrogen) using vendor's protocol. CD68 (MCA1957GA, Biorad) was used to identify macrophages. The number of EdU positive nuclei was normalized to the total number of CD68 positive macrophages in lesions. The images were taken using a Zeiss LSM 880 confocal microscope.

In vivo TUNEL assay

Male mice were fed an atherosclerotic diet for 24 weeks. After sacrificing the mice 10μm cryo-sections were prepared as described above. Apoptotic cells in the atherosclerotic lesions were detected using the Click-it Plus TUNEL Assay kit (C10617, Thermo Fischer Scientific) following the manufacturer's protocol with slight modifications. In particular, the permeabilization time was increased from 15 minutes to 20 minutes. CD68 (MCA1957GA, Biorad) antibody was used to identify the macrophages. The number of TUNEL positive nuclei was normalized to the total number of CD68 positive macrophages in the lesions. The images were taken using a Zeiss LSM 880 confocal microscope.

Isolation of bone marrow derived macrophages (BMDM)

Bone marrow (BM) cells were isolated from femurs of male wt or null mice. Cells were treated with RBC lysis buffer to remove red blood cells for five minutes, centrifuged at 364 g for 5 minutes, and re-suspended in BMDM culture medium. Culture medium consisted of high-glucose DMEM (Gibco 11965) supplemented with 10% heat inactivated fetal bovine serum (FBS), 2 mM L-glutamine, 100 units/Ml, 100 ug/Ml penicillin/streptomycin, 500 uM sodium pyruvate, and 5% v/v conditioned medium containing macrophage colony stimulating factor (M-CSF) produced by CMG cells to induce differentiation to BMDMs. BMDMs were maintained at 37° C in a humidified 5% CO_2 incubator. BMDMs were differentiated for 6 days prior to experiments, and medium was changed at day 4 of differentiation.

TLR ligand treatment of *Zhx2* wt and null BMDM

For gene expression analysis, BMDMs (from male mice) were plated at $3x10^5$ cells/well in 12-well plates. 48 hr post-planting, cells were treated with TLR-ligands (TLR1/2 - Pam3csk4 (50ng/ml), TLR3 – Poly I:C (1ug/mL), TLR4 – LPS (50 ng/mL), TLR7/8 – CL307 (100 nM), TLR9 – ODN1668 (100 nM), M1 – LPS (50 ng/mL) + IFN-y (20 ng/mL) for 8 or 24 hr in DMEM supplemented with 5% FBS, 2 mM L-glutamine, 100 units/mL, 100 ug/mL penicillin/streptomycin, 500 uM sodium pyruvate, and 5% v/v conditioned medium containing M-CSF.

For qPCR analyses, RNA was isolated with TRIzol and cDNA synthesized with high capacity cDNA reverse transcription kit. KAPA SYBR FAST qPCR master mix (2) kit and a lightCycler 480 were used for quantitative RT-PCR. Fold change related to the control was calculated using 36b as the reference gene.

For determination of proliferation, 1.45 uM of calcein-AM (final concentration) was added to each well and incubated for 15 minutes. Plates were then imaged using ImagesXpress XL (Molecular Devices). 2O high magnification fluorescence images were captured for each well (21.83% of total well surface area) using a 10x objective. Cell number was calculated using MetaXpress Software using the Multi-wavelength cell scoring module.

Immunocytochemistry of cultured cells using Ki67, EdU and TUNEL

For Ki-67 experiments: BMDM from male wt and *ZhX2* null mice were cultured in 8 wells culture slides. Cells were seeded @20,000 cells per well with 10ng/ml recombinant M-CSF.

On day 6, the cells were starved for serum and CSF-1 for 18 hours, then treated with different concentrations of mouse recombinant M-CSF (STEMCELL Technologies, Vancouver, Canada) for 48 hours. Cells were washed with PBS and fixed with 4% PFA (10min), permeabilized with 0.1% Triton X-100 (10min) and were blocked with 3%BSA and 5% goat serum (in 1X PBS) for at RT. Cells were incubated with Ki-67 (ab15580, abcam) and CD68 (MCA1957GA, Biorad) for overnight at 4°. Cells were washed and further incubated with goat anti rat, Alexa Fluor 594 (A-11007, ThermoFischerScientific) and goat anti-Rabbit, Alexa Fluor 488 (A-11008, ThermoFischerScientific) for 1 hour at room temperature. Slides were washed and mounted with DAPI (Sigma Aldrich).

For EdU staining, BMDM from male *Zhx2* wt and null mice were cultured in 8 well culture slides @20,000 cells per well with 10ng/ml of mouse recombinant M-CSF (STEMCELL Technologies). On day 6, cells were starved for serum and M-CSF for 18 hours, then treated with different concentrations of M-CSF (0, 4, 20, 100, and 500ng/ml) for 48 hours. Click-iT™ EdU Alexa Fluor™ 488 Imaging Kit (C10337, Invitrogen) was used to stain incorporated EdU following the manufacturer protocol. All images were taken using a Zeiss (Axioskop 2 plus, Carl Zeiss, Heidelberg, Germany) microscope.

For TUNEL assays, peritoneal (from female mice) and BMDM (from male mice) macrophages from *Zhx2* null and *Zhx2* wt mice were cultured as above. The apoptosis was determined by TUNEL assay using the Promega DeadEnd™ Fluorometric TUNEL System G3250 and Click-it Plus TUNEL Assay kit (C10617, Thermo Fischer Scientific), respectively. The manufacturer's protocol was followed for each kit. For some experiments, the BMDM macrophages were treated with ox-LDL (25μg/ml) or 7-ketocholesterol (40μg/ml) for 24 hours. The images were taken using Nikon (Eclipse Ti-s) and Zeiss (Axioskop 2 plus, Carl Zeiss) microscopes.

Flow cytometry

Anesthetized male mice were perfused by cardiac puncture with DPBS containing 2 mM of EDTA. Harvested aortas were digested with 250 U/mL collagenase type XI, 120 U/mL hyaluronidase type I-s, 120 U/mL DNAse1, and 450 U/mL collagenase type I (all enzymes, Sigma) in HBSS at 37 °C for 1 hour on bacterial shaker. A cell suspension was obtained by mashing the aorta through a 70-μm strainer. Cells were then stained for flow cytometry. Fcγ receptors were blocked using CD16/32 antibody for 15 min at room temperature. Surface antigens on cells were stained for 30 min at 4 °C using appropriate antibodies. Zombie Yellow™ Fixable Viability Kit (Biolegend) was used for analysis of viability, and forward- and side-scatter parameters were used for exclusion of doublets. Macrophages were identified as live, CD45+, lineage negative (CD19−, CD3 −, CD11c−), F4/80+, CD11b+, cells using a BD LSR II flowcytometer. The cell surface markers, CD86 and CD206, were used to identify M1 and M2 phenotypes, respectively. All antibodies were from Biolegend, San Diego, CA. Data were analyzed using FlowJo software.

Zhx2 ChIP-seq

Raw 264.7 macrophage cells purchased from ATCC were cultured in standard DMEM containing 10%FBS and penicillin/streptomycin at 37 degrees in 5% CO2. Cells were

transfected using Lipofectamine 2000 according to the manufacturer's protocol. For ChIP-seq experiments, mouse *Zhx2* was cloned into a pShuttle-IRES-GFP1 plasmid (ad-gene) where the C-terminal end of the gene contained a 3X-FLAG sequence.

Transfected Raw macrophages were washed 2X in cold PBS, fixed using 4% paraformaldehyde, neutralized with acid glycine then pelleted at 2million cells/pellet. These pellets were then fractionated for nuclear isolation using an NPER kit (Thermo cat# 78833). Nuclear lysate was then sonicated to ~150–300 DNA base-pair fragment size for 50min using a Bioruptor ultrasonicator (diagenode). Sonicated lysate was then subjected to ChIP using a Kit (Sigma cat #CHP-1) according to manufacturer details. Briefly, sonicated pellets were immuoprecipitated using 3ug/2million cells monoclonal FLAG antibody (Sigma cat# F3165) overnight at 4 degrees. The following day, samples were washed and cross-links reversed via incubation overnight at 65 degrees in 160 mM NaCl. Protein and RNA was then digested (Proteinase K and RNAse digestion 1hr at 37 degrees), and isolated DNA eluted using a column provided in ChIP-kit.

Isolated DNA from chromatin immunoprecipitation was subjected to library preparation using a Kappa Hyper Prep Kit (Kappa Bio cat # KK8502) according to the manufacturer's protocol. Briefly, DNA was ligated to adapters (Tru-Seq) and size-selected using AmPURE beads (Agencort cat#A63880), washed in 80% ethanol and eluted. Libraries did not require subsequent amplification and were directly sequenced. Input for sequencing was standardized and pooled at 2uL per 10nM sample measured using a Qubit fluorometric system (Thermo). The pooled sample was then sequenced in a single lane using a HiSeq4000. This pooled single lane, containing 2 replicates of ZHX2-FLAG and 1% input produced 100 million total reads

Sequencing data were downloaded, de-multiplexed and converted to FASTQ files. These files were then aligned to the mouse mm10 genome using bowtie2 [16]. The resulting SAM files were then analyzed using HOMER software [17]. Chip-Seq Plots were produced using ngsplot software and preprocessed using R Studio.

Statistical analyses

All statistical analyses were executed in the R programming environment. Two-way ANOVA or the Kruskal-Wallis test with Bonferroni correction for multiple comparisons were used to compare multiple groups. The Mann-Whitney test was used to compare two groups. Microarray results were normalized using RMA in the Affymetrix package, and differential expression p-values and Venn diagrams were calculated using the limma package. Microarray p-values were corrected using Benjamini Hochberg. $P<0.05$ was considered significant.

For analysis of lesions, a two way ANOVA was conducted to identify significant gender and genotype factors and their interactions. Prior to analysis, lesion size was adjusted in order to meet the normality and homoscedasticity assumptions. A log transformation was applied to lesion size and an outlier in the female null category was removed. For each gender by genotype category, the hypothesis of normality was not rejected using the Shapiro-Wilk statistic, and homoscedasticity was not rejected using the Levene test. Removing the single

outlier (based on a chi-square test) provides a more conservative test of the hypothesis. Including the outlier in the female null category did not change the results: sex (p = 0.00496), genotype (p = 4.41e-11), interaction (p = 0.0100).

Results

Absence of *Zhx2* expression in mice protects against atherosclerosis

When fed a Western diet, atherosclerotic lesions were markedly reduced in BALB/cJ $Ldlr^{-/-}$ mice carrying the *Zhx2* null mutation as compared to isogenic mice carrying the type wt allele (from strain BALB/cBYJ) as judged by analysis of sections from aortic root (Fig. 1A) or by *en face* analysis of the aortic arch (Fig. 1B). There was a decided sex difference, with male mice typically exhibiting about a 10-fold difference in lesion size whereas females exhibited about a 3–4-fold difference. Statistical analysis was performed using two way ANOVA to identify significant gender and genotype factors and their interactions. Following adjustment to the data to meet normality and homoscedasticity assumptions (see Methods), significant differences were observed for sex (p = 0.0061) and genotype (p = 2.3e-12). There was also a significant interaction for lesion size between gender and sex. The *Zhx2* null phenotype was largely recessive as heterozygous $Zhx2^{+/-}$ mice had lesion characteristics similar to *Zhx2* wt male mice (Fig. 1C).

We previously observed that, as compared to *Zhx2* wt mice, *Zhx2* null mice have modestly reduced levels of plasma triglycerides and cholesterol [2]. We showed that this was largely normalized when *Zhx2* was expressed specifically in liver using a transgene driven by the transthyretin promoter (TTR-Tg) [2]. On an $Ldlr^{-/-}$ background, we also observed significantly reduced levels of plasma triglycerides and cholesterol in male mice (Suppl. Fig. I.A) while the levels were not significantly different in females except for a small decrease in triglycerides (Suppl. Fig. I.B). Since these differences could contribute to the differences in atherosclerosis, we examined the effect of the TTR-Tg on plasma lipids and atherosclerosis in male $Ldlr^{-/-}$ mice. While hepatic expression of *Zhx2* increased levels of triglycerides and cholesterol in male *Zhx2* wt mice (Suppl. Fig. IC and D), it did not significantly affect atherosclerosis (Fig. I.D). Thus, it appears that the major effect of the *Zhx2* deficiency on atherosclerosis is mediated by factors independent of blood lipids.

Effect of *Zhx2* on atherosclerosis is mediated in part by bone marrow-derived cells

The lesions of *Zhx2* null mice contained reduced macrophages as compared to *Zhx2* wt mice (Fig. 2A). As judged by flow cytometry the percent macrophage (F4/80+CD11b positive) population (of the CD45+ and Lin− population) appeared to be slightly higher in wt compared to *Zhx2* null mice (p=0.06, Suppl. Fig. II). We hypothesized that Zhx2 might influence atherosclerosis by effects on bone marrow derived cells. In order to determine the contribution of hematopoietic stem cells (HSCs) arising from BM to atherosclerosis, we performed a BM transplantation study with *Zhx2* wt mice. BM was irradiated, then replaced with donor *Zhx2* wt or *Zhx2* null BM. Measurement of atherosclerotic lesion size showed more than a three-fold decrease in atherosclerosis in the wt mice transplanted with *Zhx2* null BM as compared to mice transplanted with wt BM (Fig. 2B). In experiments to determine the effect of non-HSC tissues on atherosclerosis, we transplanted *Zhx2* null BM into either

Zhx2 wt or *Zhx2* null recipients. These studies demonstrated that an approximate four-fold effect on atherosclerotic lesions size persists after normalization for BM genotype (Fig. 2C), indicating that *Zhx2* works through more than one cell system to affect atherosclerosis.

All mice in these studies were monitored by genotyping blood cells for the *Zhx2* alleles using PCR (Suppl. Fig. III). While *Zhx2* wt mice transplanted with *Zhx2* null bone marrow showed no evidence of retention in blood of the *Zhx2* wt allele, irradiated *Zhx2* null transplanted with *Zhx2* wt bone marrow consistently showed a low level of the *Zhx2* null allele (Suppl. Fig. III). Since all mice were irradiated at similar levels, in some cases in the same cages, it appears that *Zhx2* may also affect sensitivity to irradiation.

The number of monocytes and other leukocytes in the circulation did not differ significantly between *Zhx2* wt and *Zhx2* null cells on either the chow or Western diet. On the Western diet, *Zhx2* null mice appeared to have more lymphocytes (Fig. 2D). In order to identify possible differences in the differentiation of monocytes/macrophages from HSCs, we performed a colony-forming cell assay on bone marrow cells from both *Zhx2* wt and *Zhx2* null and found no differences between the two strains (Fig. 2E).

Since T cells play a significant role in atherosclerosis, including mouse models [18, 19], we performed several assays to examine effects of *Zhx2* deficiency on CD4+ T cell priming and restimulation, proliferation and suppression. All such studies were negative, as there were no significant differences between cells from *Zhx2* null as compared to *Zhx2* wt mice (Suppl. Tables I–V).

Modest effects of *Zhx2* on macrophage proliferation

To test for potential effects of *Zhx2* on macrophage proliferation, we used either immunostaining for Ki67, a marker of cell division, or incorporation of Edu. For the analysis of lesions, macrophages were identified using the markers CD68 or Mac3. In some experiments, Ki67 immunostaining suggested increased proliferation of *Zhx2* wt as compared to null macrophages, although the small size of lesions in *Zhx2* null mice made quantitation difficult (Suppl. Figs. IV.A and B). More consistent results were obtained using EdU incorporation, which showed a trend toward increased proliferation in wt mice (Suppl. Figs. IV.C and D).

In order for more accurately assess *Zhx2* effects on proliferation, we examined cultured BM-derived macrophages and again assessed proliferation using Ki67 or EdU incorporation. We preformed the experiments at varying concentrations of M-CSF, a key driver of macrophage proliferation. At low M-CSF concentrations, no differences were observed but at higher concentrations *Zhx2* wt macrophages showed a slight increase in proliferation (Suppl. Figs. IV.E, F, G, H). The effective concentration of M-CSF in lesions is unknown. As discussed below, *Zhx2* genotype did not affect the proliferation of BM-derived macrophages in response to a variety of TLR ligands.

Zhx2 null mice exhibit increased apoptosis in lesions and *in vitro*

The effects of *Zhx2* in apoptosis were examined using TUNEL assay. Lesional macrophages were identified using the marker CD68. Figure 3A shows representative sections of *Zhx2* wt

and null lesions immunostained with antibodies to CD68 and TUNEL. The fraction of double positive cells indicated that the level of apoptosis in *Zhx2* null was dramatically increase as compared to wt (Fig. 3B).

To confirm these findings and further examine the underlying mechanism, we quantitated apoptosis in cultured BM-derived macrophages (BMDM) and peritoneal macrophages. Using TUNEL staining, BMDM from *Zhx2* null mice showed an approximately 2-fold increase in apoptosis (Fig. 3C and D). In $Ldlr^{-/-}$ mice maintained on a Western diet, peritoneal macrophages from *Zhx2* null mice showed an approximately 3-fold increase of apoptosis as compared to macrophages from *Zhx2* wt mice (Fig. 3E and F). In contrast, peritoneal macrophages from mice maintained on a chow diet exhibited little or no difference in apoptosis (Fig. 3E and F). Thus, there appears to be an interaction between the expression of *Zhx2* and cholesterol loading with respect to macrophage apoptosis. We also performed the TUNEL assay on BMDM treated with ox-LDL or 7-ketocholesterol. The effect of *Zhx2* genotype was similar in each of the experiments (Fig. 3C)

Zhx2 regulation and effects on gene expression in macrophages

Macrophages from *Zhx2* wt and *Zhx2* null mice on a BALB/cJ, $Ldlr^{-/-}$ background were isolated, cultured, and a subset treated with bacterial lipopolysaccharide (LPS). Macrophages isolated from *Zhx2* wt mice showed an increase of approximately 8-fold in *Zhx2* transcript levels after LPS treatment in male mice (Fig. 3G). Similar studies in macrophages from a panel of inbred mouse strains on a chow diet [20] showed only modest variation in *Zhx2* basal levels (with the exception of BALB/cJ) but wide variation in response to LPS treatment (Suppl. Table VI), ranging from no induction in the $TLR4^{-/-}$ strains such as C3H/HeJ to 24-fold in strain AxB-10 (Suppl. Table VI).

To examine the effect of *Zhx2* deficiency on gene expression, thioglycollate-induced peritoneal macrophages were isolated from male and female chow-fed *Zhx2* wt and *Zhx2* null mice. The expression profiles were determined by microarray analysis and differentially expressed transcripts were identified by comparing the wt to null expression data. Nearly 1400 probes were differentially expressed between macrophages isolated from chow-fed *Zhx2* wt and *Zhx2* null mice, in both males and females (Suppl. Table VII). Of the genes differentially expressed among both sexes, approximately 600 were regulated more than two-fold, with some genes being differentially expressed over 100-fold. The top differentially expressed genes were all repressed in the presence of *Zhx2*. Gene ontology analysis performed on these genes identified the immune response category as the most enriched in the dataset, with a corrected p-value of 2.0×10^{-25} (Suppl. Table VIII). Other notable significantly enriched GO categories include antigen presentation and apoptosis.

Given that the status of macrophage polarization has been demonstrated as an important contributing factor to atherosclerosis [21], we also asked if there was significant enrichment of M1 or M2 macrophage markers between *Zhx2* wt and *Zhx2* null mice. Of the 743 genes significantly enriched in the wt mice, 37% of the genes have been annotated as M1 macrophage markers [22], whereas less than 5% of marker genes were enrichmed in the null group (Suppl. Table VIII). Conversely, 42% of the genes upregulated in *Zhx2* null macrophages have been annotated as M2 macrophage markers (Suppl. Table VIII). These

data suggest a role of *Zhx2* in promoting gene expression signatures, consistent with M1 macrophage polarization.

To further examine this, we performed flow cytometric analysis on lesional macrophages from mice fed an atherogenic diet using specific markers for M1 (CD86) and M2 (CD206). A significantly higher percentage of CD86 positive cells was observed in *Zhx2* wt compared to null mice consistent with the conclusion that *Zhx2* promotes an M1 phenotype (Fig. 3H).

We also examined the effect of *Zhx2* genotype on responses to a variety of TLR ligands, including TLR1/2, TLR3, TLR4, TLR7/8, TLR9, and the M1 inducer LPS + interferon gamma. BM-derived macrophages were plated at various densities and proliferation following the treatments was assessed as previously described [23] (Suppl. Fig. V). In general, TLR stimulation inhibited the growth of *Zhx2* wt and null cells to the same extent, similar to treatment of BM-derived macrophages from C57BL/6J mice. We also examined the expression of several proinflammatory cytokines and chemokines (IL-1b, IL-12b, TNF-a, and Cxcl 10) following treatment with TLR ligands. Effects were negligible or modest (Suppl. Fig. V).

Chip-Seq analysis

Efforts to carry out global analysis of *Zhx2* binding to chromatin using antibodies have previously been unsuccessful. Therefore, we tagged *Zhx2* with a 3X-FLAG at the carboxyl terminus and showed that it remained active, as judged by changes in gene expression, when transfected into the RAW mouse macrophage cell line (see Methods). To perform ChIP-seq, the FLAG-tagged *Zhx2* was overexpressed in RAW macrophages, then subjected to cross-linking, immunoprecipitation and subsequent sequencing of bound DNA. We detected significant enrichment of 5,402 peaks (5% FDR and > 2-fold enrichment over input). The locations of the peaks with respect to genes are summarized in Suppl. Table IX. To further refine our analysis, we chose to focus on regions which were <1MB from a coding gene and achieved a highly stringent level of significance (1%FDR and > 4-fold enrichment over input). We narrowed this list to 384 total peaks which met this criterion. Pathway enrichment of this list of genes alone was not highly-informative as to the function of the protein. To gain a more comprehensive snapshot of *Zhx2* function, we overlapped macrophage genes which showed stringent *Zxh2* ChIP-seq enrichment and induction of expression in the *Zhx2* null vs wt macrophage gene expression. Roughly half of the 384 genes from the ChIP-Seq analysis also showed significant induction in the null vs wt macrophages (>2-fold increase), indicating substantial functional overlap ($p<10^{-6}$) between ChIP-Seq and expression arrays (Suppl. Table X). We observed significant enrichment for transcriptional repression, as well as apoptosis, suggesting *Zhx2* binds DNA to repress expression of apoptosis genes in macrophages (Suppl. Table XI). Two known regulators of apoptosis, Jun [24, 25] and Bcl6 [26, 27], which showed overlap in this analysis are shown in Figure 4A. It is noteworthy that Bcl6 is khown to repress inflammation and atherosclerosis [28].

We also performed motif enrichment on the Chip-seq data. The top-ranked candidate based on motif enrichment was the transcriptional repressor Yin-Yang-1 (Fig 4B). While Yin Yang 1 (YY1) has been implicated in many biologic processes, several studies have observed a

robust capacity of the transcriptional repressor to suppress expression of apoptotic genes [29, 30], offering further evidence of overlapping roles of *Zhx2* and YY1.

Discussion

Our studies reveal a dramatic effect of *Zhx2* expression on atherosclerosis development in the *Ldlr*$^{-/-}$ mouse model. Strain BALB/cJ mice have long been known to be particularly resistant to atherosclerosis [31] and our study now shows that this is largely due to the mutation in *Zhx2* (Fig. 1). We previously showed that hepatocyte-specific expression of *Zhx2* using a transgene driven by a transthyretin promoter normalized plasma lipids and we observed that the transgene does not significantly affect atherosclerosis. Thus, the susceptibility to atherosclerosis appears to be largely independent of the effects of *Zhx2* on plasma lipids, α-fetoprotein or expression in liver. Because *Zhx2* is expressed in most cell types, including bone marrow-derived cells and vascular cells, the cell types critical for lesion development were unclear. In the absence of cell-specific *Zhx2* null mice, we decided to carry out bone marrow transplantation experiments, and these revealed that the atherosclerosis phenotype is partially mediated by BM derived cells, presumably macrophages or lymphocytes (Fig. 2). Leukocyte levels were not affected by the *Zhx2* mutation, nor did we observe any significant differences in monocyte or lymphocyte characteristics. We carried out a series of studies to examine lymphocyte immune functions but failed to identify any effects of *Zhx2* deficiency (Suppl. Tables I–V). To examine whether the effect of *Zhx2* expression on atherosclerosis was related to macrophage functions, we quantitated both macrophage proliferation and apoptosis in lesions. The *Zhx2* null mice exhibited only modestly reduced proliferation (Suppl. Figs. III.A–H) but significantly increased apoptosis, both *in vitro* and in lesions, as judged by TUNEL staining (Fig. 3A–F). To examine the mechanisms by which *Zhx2* affects macrophage functions, we carried out analysis of the effects of *Zhx2* on global transcript levels and also performed ChIP-seq analyses to identify the direct targets of *Zhx2*. We also examined the expression of M1/M2 markers and the responses to inflammatory ligands. The results support a role of *Zhx2* in macrophage apoptosis and suggest that *Zhx2* expression promotes inflammatory functions (Fig. 4).

We originally identified the *Zhx2* locus on mouse chromosome 15 using quantitative trait locus mapping of a cross between inbred strains BALB/cJ and MRL/*lpr* [1] and, subsequently, isolated the locus as a congenic region on a BALB/cJ background [3]. We then performed crosses to narrow the locus to about a dozen genes and then examined these one-by-one, revealing that *Zhx2* for strain BALB/cJ exhibited dramatically reduced expression due to a retroviral insertion [2]. During the course of these studies, we carried out a preliminary investigation of the potential impact of the *Zhx2* null allele on atherosclerosis using a cholic acid-containing diet [31] and observed a decrease as compared to the wt allele. To explore this further, we have now introduced the wt allele from the closely related strain BALB/cByJ onto a BALB/cJ background and have introduced an *Ldlr*$^{-/-}$ targeted gene mutation onto both the *Zhx2* null and *Zhx2* wt BALB/cJ backgrounds. On this background, we observed a dramatic impact of *Zhx2* on lesion development, with *Zhx2* null mice protected by about 10-fold in males and 3- to 4-fold in females (Fig. 1).

Zhx2 appears to be a transcriptional repressor, originally shown to be involved in the modulation of α-fetoprotein expression in newborn mice [4]. Using microarrays, we examined the effects of *Zhx2* deficiency in peritoneal macrophages. Expression levels of hundreds of genes were significantly affected and the differentially expressed gene set was significantly enriched for immune response genes, including apoptosis. Consistent with this, we observed a striking induction of *Zhx2* in response to the pro-inflammatory stimulus LPS, which induces an inflammatory response in macrophages through the activation of the TLR4 receptor. Recent studies describe downstream TLR4 activation of XBP1, a potent transcriptional activator [32]. Separate studies on a Hodgkin lymphoma cell line identified a chromosomal rearrangement that represses *Zhx2* expression [7] and a further study suggested that these mutations prevented the binding of XBP1 to the *Zhx2* regulatory region [6]. These findings are consistent with a hypothesis of LPS regulation of *Zhx2* through the *Tlr4-Xbp1* pathways. In addition to our data on the role of *Zhx2* in macrophages, recent studies have described a role for *Zhx2* in other leukocytes [6, 8, 9] and in adaptive immunity [33], indicating multiple roles for *Zhx2* in bone marrow derived cells of the immune system. The available antibodies to *Zhx2* exhibited significant non-specific binding and thus we were unable to determine whether *Zhx2* was upregulated in lesions.

We were successful in a global analysis of *Zhx2* targets using ChIP-seq analysis. We used a macrophage cell line, given the evidence that the effect of *Zhx2* deficiency on atherosclerosis is mediated in part by bone marrow-derived macrophages. It is likely that the chromatin interactions of *Zhx2* would differ in other cell types; for example, *Zhx2* is clearly involved in the repression of α-fetoprotein and, yet, we observed no significant enrichment of sequences near the gene in macrophages. It is possible, of course, that the repression of α-fetoprotein represents a secondary effect. The ChIP-seq results showed very significant overlap with the expression data obtained by comparing *Zhx2* wt with *Zhx2* null macrophages. Both datasets are consistent with a role in apoptosis of macrophages. Additionally, expression array data suggested a role for *Zhx2* in regulation of macrophage polarization, specifically promoting an M1 pro-inflammatory transcriptional signature. A role in inflammatory functions is also suggested by the finding that *Zhx2* is induced by LPS treatment (Fig. 3H).

A pro-apoptotic role of *Zhx2* would be consistent with its role as a tumor suppressor in lymphomas and myelomas, where a deficiency of *Zhx2* has been associated with cancer [6, 8]. This contrasts to the situation in macrophages, where *Zhx2* deficiency promotes apoptosis and reduces the development of atherosclerotic lesions. Although we observe strong evidence for a role of *Zhx2* in macrophage survival, our bone marrow studies indicate that effects in non-bone marrow-derived cells explain a significant fraction of the effect on atherosclerosis. *Zhx2* is expressed in both endothelial cells and smooth muscle cells [34]. As it has also been described as a developmental repressor in the liver [35] and brain [36], it is possible that activity of the gene can affect disease pathology in a variety of tissues.

Our results may also be relevant to the recent findings that clonal hematopoiesis can increase risk of atherosclerosis, since a likely mechanism involves increased macrophage proliferation or apoptosis in lesions [37, 38] It is also clear that non-BM derived cells contribute to the effects of *Zhx2* on atherosclerosis, and we have not definitively ruled out

the possibility that BM-derived cells other than macrophages contribute. Our results are also of potential relevance to the finding that a locus containing the *Zhx2* gene was significantly associated with coronary intima media thickness, a subclinical measure of atherosclerosis, in a genome-wide association study. However, no evidence of significant association of the locus was observed in large association studies for other cardiovascular disease traits [39–41]

A number of important questions remain to be answered. The mechanisms by which *Zhx2* affects macrophage apoptosis and inflammation are unclear. As a transcription factor with broad effects, it is likely to influence a variety of relevant pathways. Also, the effects of *Zhx2* on atherosclerosis are clearly mediated in part by non-BM-derived cells, and the identify of these cells is unknown. This issue can probably be best pursued using tissue-specific modulation of *Zhx2* expression. Finally, we have performed only the initial characterization of the genomic targets of *Zhx2* and its interactions with other transitional regulators. For example, it is known to form heterodimers with other members of the zinc finger and homeoboxes family.

Supplementary Material

Refer to Web version on PubMed Central for supplementary material.

Acknowledgments

a) Acknowledgements: A.E., R.P., M.S., X.W., M.M., S.B., S.S., and A.J.L. designed the studies. All others performed experiments. The manuscript was written by A.J.L., A.E., and S.S., and was reviewed by all authors. We thank Rita Cantor and Calvin Pan for help with statistical analyses.

b) Sources of Funding: This work was supported by NIH grant HL30568 (A.J.L), NIH HL138193 (M.M.S.), NIH T32HL69766 (M.M.S.), and the Foundation Leducq. X.W. and M.M.S. were also supported by NIH training grant T32HL007895.

c) Disclosures: None

Nonstandard abbreviations and acronyms

AFP	Alpha-fetoprotein
BMDM	Bone marrow derived macrophages
DCs	Dendritic cells
EdU	5-Ethynyl-2′-deoxyuridine
LPS	Lipopolysaccharide
Ldlr$^{-/-}$	Low density lipoprotein receptor null
M-CSF	Macrophage colony stimulating factor
Treg	Regulatory T-cells
TTR-Tg	Transthyretin promoter
wt	Wild type

References

1. Gu L, Johnson MW, Lusis AJ. Quantitative trait locus analysis of plasma lipoprotein levels in an autoimmune mouse model : interactions between lipoprotein metabolism, autoimmune disease, and atherogenesis. Arterioscler Thromb Vasc Biol. 1999; 19:442–453. [PubMed: 9974430]
2. Gargalovic PS, Erbilgin A, Kohannim O, Pagnon J, Wang X, Castellani L, LeBoeuf R, Peterson ML, Spear BT, Lusis AJ. Quantitative trait locus mapping and identification of Zhx2 as a novel regulator of plasma lipid metabolism. Circ Cardiovasc Genet. 2010; 3:60–67. [PubMed: 20160197]
3. Wang X, Gargalovic P, Wong J, Gu JL, Wu X, Qi H, Wen P, Xi L, Tan B, Gogliotti R, Castellani LW, Chatterjee A, Lusis AJ. Hyplip2, a new gene for combined hyperlipidemia and increased atherosclerosis. Arterioscler Thromb Vasc Biol. 2004; 24:1928–1934. [PubMed: 15331434]
4. Perincheri S, Dingle RW, Peterson ML, Spear BT. Hereditary persistence of alpha-fetoprotein and H19 expression in liver of BALB/cJ mice is due to a retrovirus insertion in the Zhx2 gene. Proc Natl Acad Sci U S A. 2005; 102:396–401. [PubMed: 15626755]
5. Yue X, Zhang Z, Liang X, Gao L, Zhang X, Zhao D, Liu X, Ma H, Guo M, Spear BT, Gong Y, Ma C. Zinc fingers and homeoboxes 2 inhibits hepatocellular carcinoma cell proliferation and represses expression of Cyclins A and E. Gastroenterology. 2012; 142:1559–1570. [PubMed: 22406477]
6. Nagel S, Schneider B, Meyer C, Kaufmann M, Drexler HG, Macleod RA. Transcriptional deregulation of homeobox gene ZHX2 in Hodgkin lymphoma. Leuk Res. 2012; 36:646–655. [PubMed: 22078940]
7. Nagel S, Schneider B, Rosenwald A, Meyer C, Kaufmann M, Drexler HG, MacLeod RA. t(4;8)(q27;q24) in Hodgkin lymphoma cells targets phosphodiesterase PDE5A and homeobox gene ZHX2. Genes Chromosomes Cancer. 2011; 50:996–1009. [PubMed: 21987443]
8. Legartova S, Harnicarova-Horakova A, Bartova E, Hajek R, Pour L, Kozubek S. Expression of RAN, ZHX-2, and CHC1L genes in multiple myeloma patients and in myeloma cell lines treated with HDAC and Dnmts inhibitors. Neoplasma. 2010; 57:482–487. [PubMed: 20568903]
9. Armellini A, Sarasquete ME, Garcia-Sanz R, et al. Low expression of ZHX2, but not RCBTB2 or RAN, is associated with poor outcome in multiple myeloma. Br J Haematol. 2008; 141:212–215. [PubMed: 18353163]
10. Kawata H, Yamada K, Shou Z, Mizutani T, Yazawa T, Yoshino M, Sekiguchi T, Kajitani T, Miyamoto K. Zinc-fingers and homeoboxes (ZHX) 2, a novel member of the ZHX family, functions as a transcriptional repressor. Biochemical J. 2003; 373:747–757.
11. Mehrabian M, Qiao JH, Hyman R, Ruddle D, Laughton C, Lusis AJ. Influence of the apoA-II gene locus on HDL levels and fatty streak development in mice. Arterioscler Thromb. 1993; 13:1–10. [PubMed: 8422330]
12. Shih DM, Xia YR, Wang XP, Miller E, Castellani LW, Subbanagounder G, Cheroutre H, Faull KF, Berliner JA, Witztum JL, Lusis AJ. Combined serum paraoxonase knockout/apolipoprotein E knockout mice exhibit increased lipoprotein oxidation and atherosclerosis. J Biol Chem. 2000; 275:17527–17535. [PubMed: 10748217]
13. Wang SS, Martin LJ, Schadt EE, Meng H, Wang X, Zhao W, Ingram-Drake L, Nebohacova M, Mehrabian M, Drake TA, Lusis AJ. Disruption of the aortic elastic lamina and medial calcification share genetic determinants in mice. Circ Cardiovasc Genet. 2009; 2:573–582. [PubMed: 20031637]
14. Daugherty A, Tall AR, Daemen M, Falk E, Fisher EA, Garcia-Cardena G, Lusis AJ, Owens AP 3rd, Rosenfeld ME, Virmani R. American Heart Association Council on Arteriosclerosis T, Vascular B, Council on Basic Cardiovascular S. Recommendation on Design, Execution, and Reporting of Animal Atherosclerosis Studies: A Scientific Statement From the American Heart Association. Arterioscler Thromb Vasc Biol. 2017; 37:e131–e157. [PubMed: 28729366]
15. Franken NA, Rodermond HM, Stap J, Haveman J, van Bree C. Clonogenic assay of cells in vitro. Nat Protoc. 2006; 1:2315–2319. [PubMed: 17406473]
16. Langmead B, Salzberg SL. Fast gapped-read alignment with Bowtie 2. Nat Methods. 2012; 9:357–359. [PubMed: 22388286]
17. Heinz S, Benner C, Spann N, Bertolino E, Lin YC, Laslo P, Cheng JX, Murre C, Singh H, Glass CK. Simple combinations of lineage-determining transcription factors prime cis-regulatory

elements required for macrophage and B cell identities. Mol Cell. 2010; 38:576–589. [PubMed: 20513432]

18. Tabas I, Garcia-Cardena G, Owens GK. Recent insights into the cellular biology of atherosclerosis. J Cell Biol. 2015; 209:13–22. [PubMed: 25869663]
19. Hansson GK, Hermansson A. The immune system in atherosclerosis. Nat Immunol. 2011; 12:204–212. [PubMed: 21321594]
20. Orozco LD, Bennett BJ, Farber CR, et al. Unraveling inflammatory responses using systems genetics and gene-environment interactions in macrophages. Cell. 2012; 151:658–670. [PubMed: 23101632]
21. Mills CD, Ley K. M1 and M2 macrophages: the chicken and the egg of immunity. J Innate Immun. 2014; 6:716–726. [PubMed: 25138714]
22. Buscher K, Ehinger K, Gupta P, Pramod AB, Wolf D, Tweet G, Pan C, Mills CD, Lusis AJ, Ley K. Natural variation of macrophage activation as disease-relevant phenotype predictive of inflammation and cancer survival. Nat Commun. 2017; 8:16041. [PubMed: 28737175]
23. York AG, Williams KJ, Argus JP, et al. Limiting Cholesterol Biosynthetic Flux Spontaneously Engages Type I IFN Signaling. Cell. 2015; 163:1716–1729. [PubMed: 26686653]
24. Bossy-Wetzel E, Bakiri L, Yaniv M. Induction of apoptosis by the transcription factor c-Jun. EMBO J. 1997; 16:1695–1709. [PubMed: 9130714]
25. Shaulian E, Karin M. AP-1 as a regulator of cell life and death. Nat Cell Biol. 2002; 4:E131–136. [PubMed: 11988758]
26. Kumagai T, Miki T, Kikuchi M, Fukuda T, Miyasaka N, Kamiyama R, Hirosawa S. The proto-oncogene Bc16 inhibits apoptotic cell death in differentiation-induced mouse myogenic cells. Oncogene. 1999; 18:467–475. [PubMed: 9927203]
27. Kurosu T, Fukuda T, Miki T, Miura O. BCL6 overexpression prevents increase in reactive oxygen species and inhibits apoptosis induced by chemotherapeutic reagents in B-cell lymphoma cells. Oncogene. 2003; 22:4459–4468. [PubMed: 12881702]
28. Barish GD, Yu RT, Karunasiri MS, et al. The Bcl6-SMRT/NCoR cistrome represses inflammation to attenuate atherosclerosis. Cell Metab. 2012; 15:554–562. [PubMed: 22465074]
29. Krippner-Heidenreich A, Walsemann G, Beyrouthy MJ, Speckgens S, Kraft R, Thole H, Talanian RV, Hurt MM, Luscher B. Caspase-dependent regulation and subcellular redistribution of the transcriptional modulator YY1 during apoptosis. Mol Cell Biol. 2005; 25:3704–3714. [PubMed: 15831475]
30. Trabucco SE, Gerstein RM, Zhang H. YY1 Regulates the Germinal Center Reaction by Inhibiting Apoptosis. J Immunol. 2016; 197:1699–1707. [PubMed: 27448584]
31. Paigen B, Mitchell D, Reue K, Morrow A, Lusis AJ, LeBoeuf RC. Ath-1, a gene determining atherosclerosis susceptibility and high density lipoprotein levels in mice. Proc Natl Acad Sci USA. 1987; 84:3763–3767. [PubMed: 3473481]
32. Martinon F, Chen X, Lee AH, Glimcher LH. TLR activation of the transcription factor XBP1 regulates innate immune responses in macrophages. Nat Immunol. 2010; 11:411–418. [PubMed: 20351694]
33. Ovsyannikova IG, Kennedy RB, O'Byrne M, Jacobson RM, Pankratz VS, Poland GA. Genome-wide association study of antibody response to smallpox vaccine. Vaccine. 2012; 30:4182–4189. [PubMed: 22542470]
34. Erbilgin A, Civelek M, Romanoski CE, Pan C, Hagopian R, Berliner JA, Lusis AJ. Identification of CAD candidate genes in GWAS loci and their expression in vascular cells. J Lipid Res. 2013; 54:1894–1905. [PubMed: 23667179]
35. Perincheri S, Dingle RW, Peterson ML, Spear BT. Hereditary persistence of alpha-fetoprotein and H19 expression in liver of BALB/cJ mice is due to a retrovirus insertion in the Zhx2 gene. Proc Natl Acad Sci USA. 2005; 102:396–401. [PubMed: 15626755]
36. Wu C, Qiu R, Wang J, Zhang H, Murai K, Lu Q. ZHX2 Interacts with Ephrin-B and regulates neural progenitor maintenance in the developing cerebral cortex. J Neurosci. 2009; 29:7404–7412. [PubMed: 19515908]

37. Fuster JJ, MacLauchlan S, Zuriaga MA, et al. Clonal hematopoiesis associated with TET2 deficiency accelerates atherosclerosis development in mice. Science. 2017; 355:842–847. [PubMed: 28104796]

38. Jaiswal S, Natarajan P, Silver AJ, et al. Clonal hematopoiesis and risk of atherosclerotic cardiovascular disease. N Engl J Med. 2017; 377:111–121. [PubMed: 28636844]

39. Braenne I, Civelek M, Vilne B, et al. Prediction of Causal Candidate Genes in Coronary Artery Disease Loci. Arterioscler Thromb Vasc Biol. 2015; 35:2207–2217. [PubMed: 26293461]

40. LeBlanc M, Zuber V, Andreassen BK, et al. Identifying novel gene variants in coronary artery disease and shared genes with several cardiovascular risk factors. Circ Res. 2016; 118:83–94. [PubMed: 26487741]

41. Bis JC, Kavousi M, Franceschini N, et al. Meta-analysis of genome-wide association studies from the CHARGE consortium identifies common variants associated with carotid intima media thickness and plaque. Nat Genet. 2011; 43:940–947. [PubMed: 21909108]

Highlights

- BALB/cJ mice are resistant to atherosclerosis due to a naturally occurring null mutation of the transcription factor *Zhx2*
- The effect of *Zhx2* on atherosclerosis is mediated in part by bone marrow-derived cells
- *Zhx2* deficiency reduces macrophage proliferation and increases macrophage apoptosis in lesions
- ChIP-seq and global expression analyses indicate that *Zhx2* influences apoptosis and growth genes

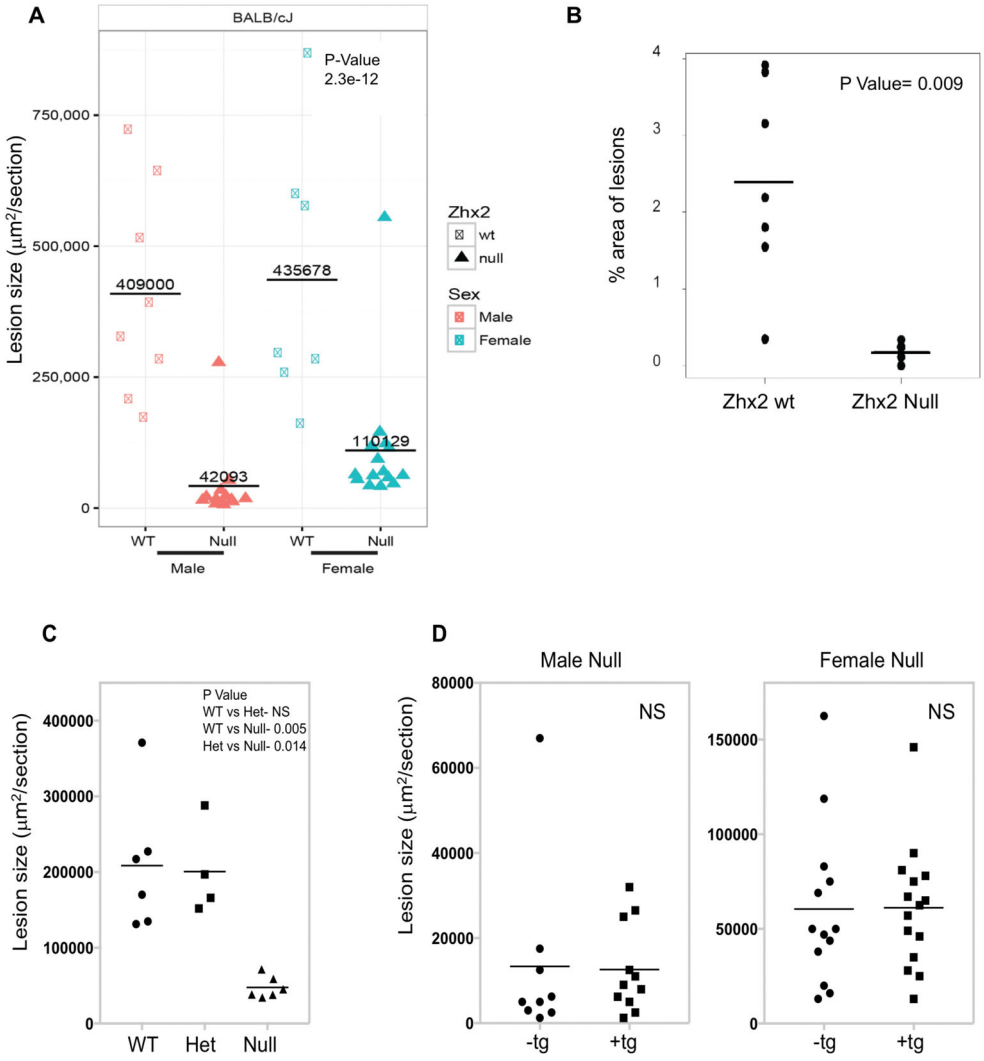

Figure 1. *Zhx2* deficiency suppresses atherosclerosis in BALB/cJ *Ldlr*$^{-/-}$ mice independently of expression in liver or effects on plasma lipids

(A) *Ldlr*$^{-/-}$ *Zhx2* wt and *Zhx2* null mice on a BALB/cJ *Ldlr*$^{-/-}$ background were maintained on a Western diet for 18 weeks and atherosclerotic lesions were quantitated. Aortic root measurements for male and female mice of both genotypes are shown (n=7–15). (B) *En face* atherosclerosis measurements for male *Zhx2* wt (n=7) and *Zhx2* null (n=4) mice on a BALB/cJ, *Ldlr*$^{-/-}$ background. (C) Male BALB/cJ *Ldlr*$^{-/-}$ mice of *Zhx2* genotypes +/+, +/−, −/− were maintained on a Western diet for 18 weeks and lesions were quantitated (± SEM). (D) Atherosclerosis in male *Ldlr*$^{-/-}$, *Zhx2* null mice is not significantly altered by transgenic (Tg) expression of *Zhx2* in liver using a transthyretin (TTR) promoter.

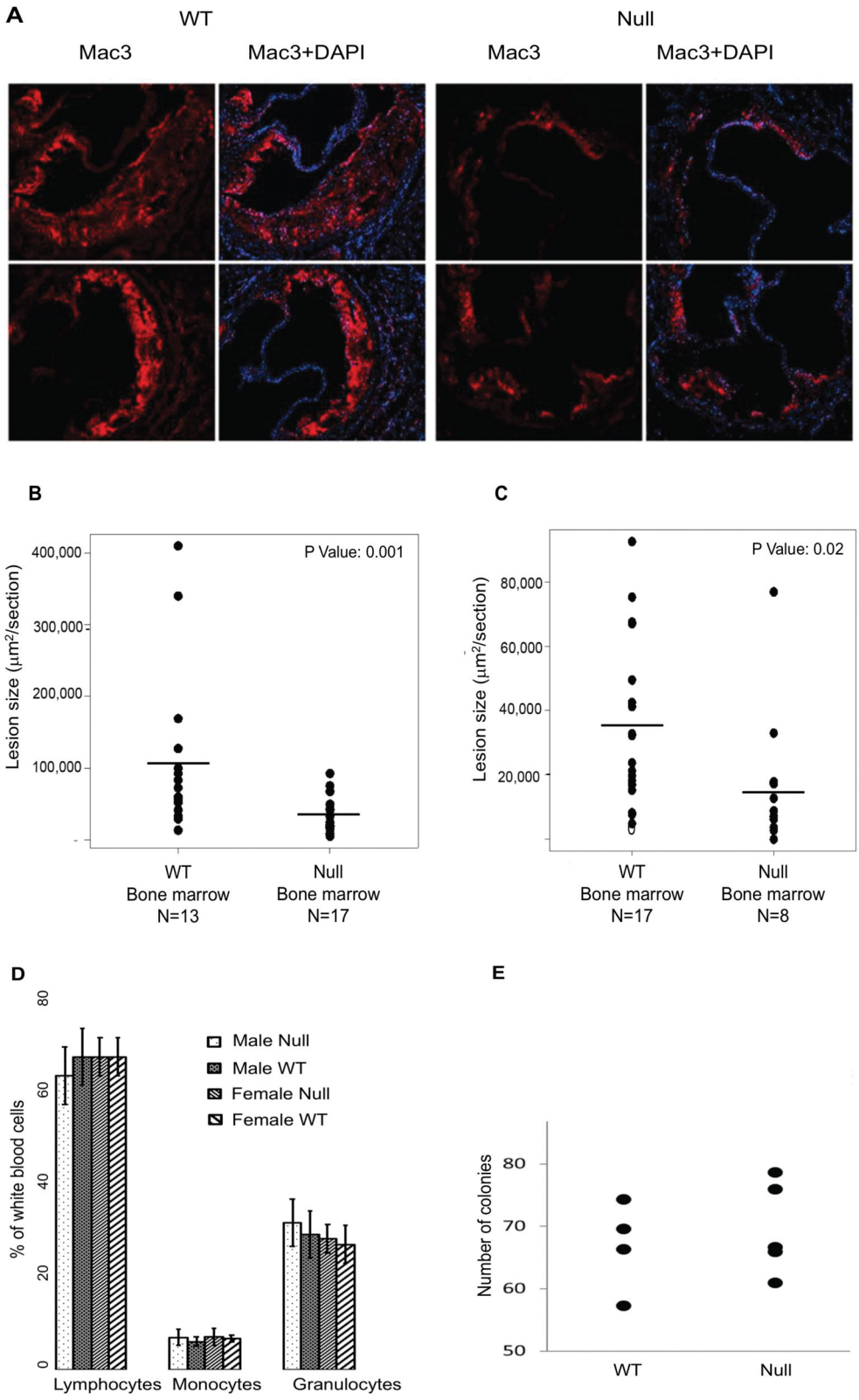

Figure 2. The effects of *Zhx2* on atherosclerosis are mediated in part by bone marrow-derived cells

(A): Representative images of immunostaining of lesion macrophages. Red: Mac3; Blue, DAPI. Original magnification, 10× (B): Aortic root lesions of BALB/cJ *Ldlr*$^{-/-}$ *Zhx2* wt or *Zhx2* null bone marrow transplants into *Ldlr*$^{-/-}$ *Zhx2* wt (C): Aortic root lesions of *Ldlr*$^{-/-}$ *Zhx2* null bone marrow transplants into *Ldlr*$^{-/-}$ *Zhx2* wt or *Zhx2* null recipients (D): Circulating leukocyte levels in *Zhx2* null and wt mice on a Western diet were examined using a HemaTrue analyzer. Shown is a representative experiment (N=7–11 mice per condition, $\pm$ SD). (E): The number of committed bone marrow stem cells responsive to M-CSF did not differ between *Zhx2* null and *Zhx2* wt mice.

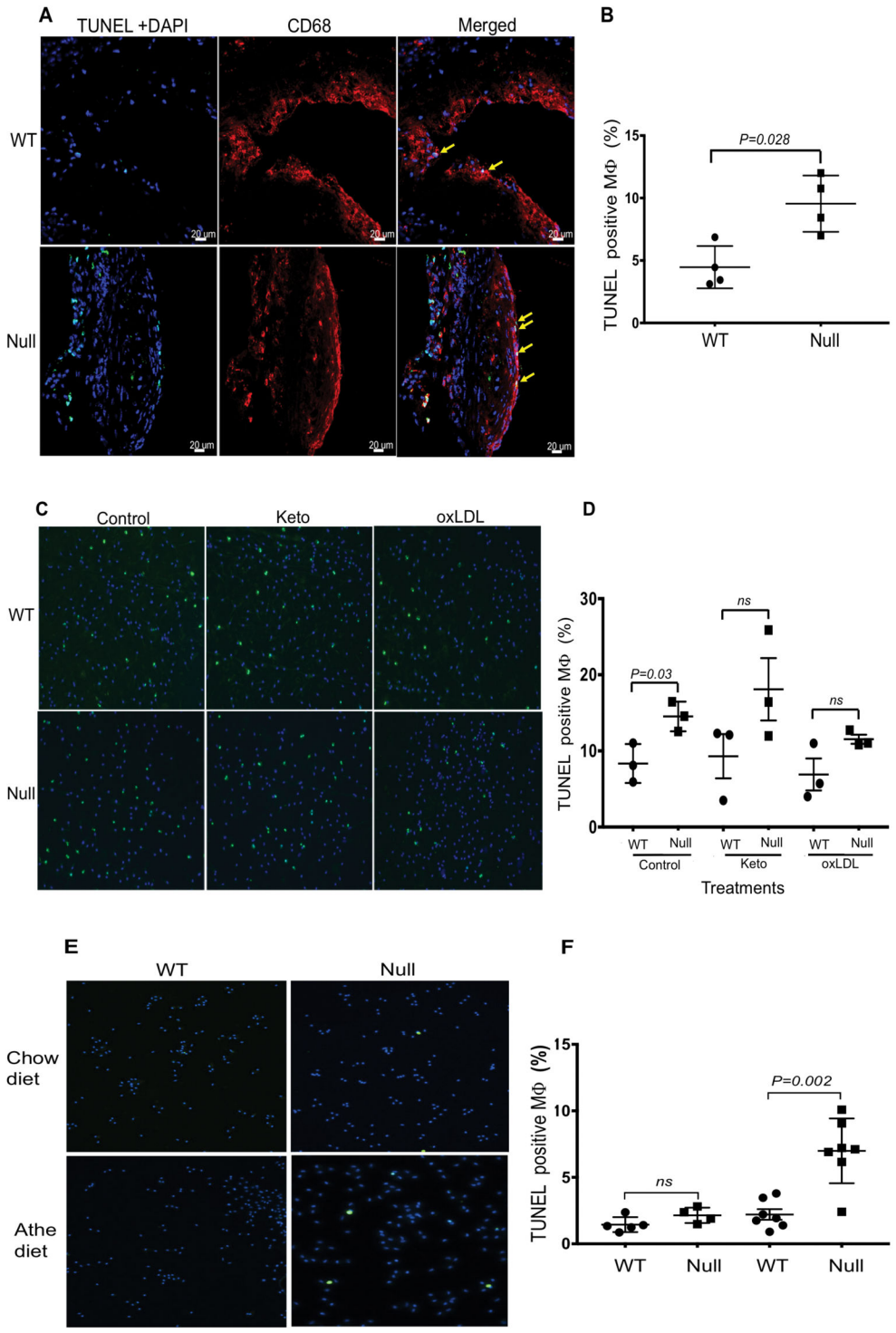

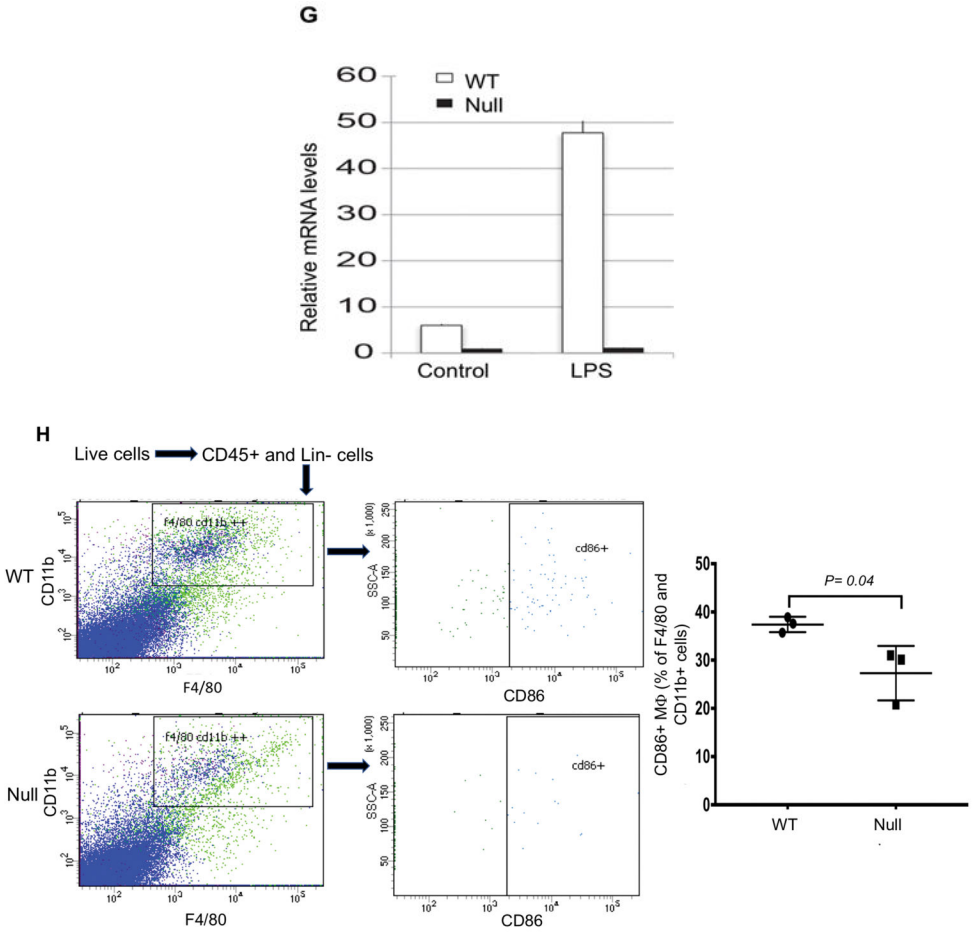

Figure 3. *Zhx2* deficiency promotes macrophage apoptosis and an M2 phenotype *in vitro* and in lesions

(A) Representative sections of lesions from *ZhX2* wt (top) and *ZhX2* null (bottom) mice stained for TUNEL or CD68. The last panel shows the merged image, magnification X20 (B) Quantitation of TUNEL positive macrophages in lesions (n=4 mice). (C) *In vitro* TUNEL assay in cultured BMDM from *Zhx2* wt and null macrophages with and without oxidized LDL (oxLDL) and 7-ketocholesterol (Keto). (D) Quantitation of TUNEL positive macrophages *in vitro* with and without oxLDL and Keto (n=3 mice, 4–5 observation from each mice). (E) *In vitro* apoptosis by TUNEL assay of peritoneal macrophages isolated from the mice maintained on chow or Western diets. (F) Quantitation of TUNEL positive peritoneal macrophages (n= 4 mice, 1–2 observation from each mice) (G) Peritoneal macrophages from BALB/cJ, $Ldlr^{-/-}$ male mice were treated with bacterial lipopolysaccharide (LPS) and *Zhx2* transcript levels quantitated by quantitative PCR. (H)Lesional macrophages for *Zhx2* wt and null mice were examined for M1 markers using flow cytometry. A significantly higher percentage of cells expressed the M1 marker CD86 (n= 4 mice, aorta from 2 mice were combined in each group).

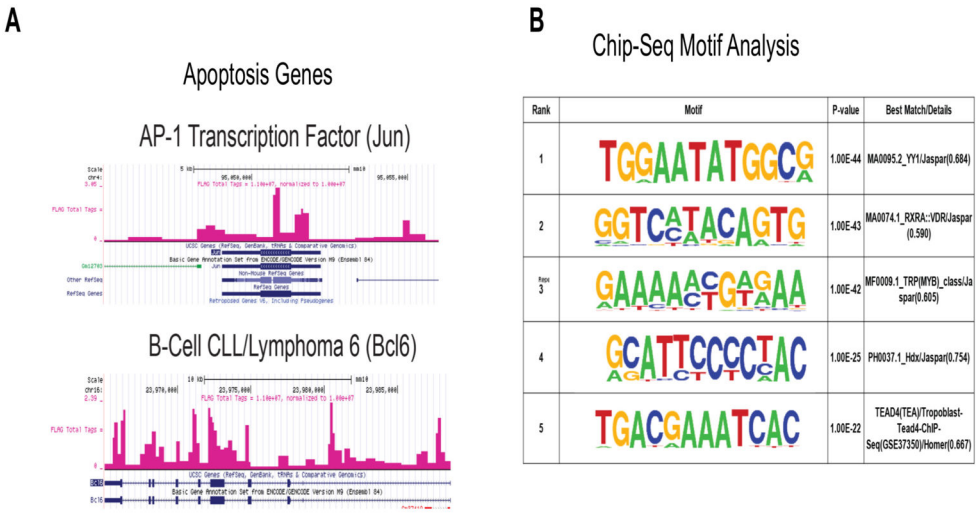

Figure 4. ChIP-seq analysis of *Zhx2* in the RAW macrophage cell line

(A) Examples of enrichment of ChIP-seq peaks at two genes in *Jun* and *Bcl6*. (B) Transcription factor motifs enriched in *Zhx2* ChIP-seq peaks, including p-values and best match details.